symmetry

IMPACT FACTOR 2.940

CITESCORE 4.3

Article

Circuit Complexity in Interacting Quenched Quantum Field Theory

Sayantan Choudhury, Rakshit Mandish Gharat, Saptarshi Mandal and Nilesh Pandey

Special Issue
Symmetry and Asymmetry in Quantum Mechanics

Edited by
Dr. Valeriy Sbitnev

MDPI

https://doi.org/10.3390/sym15030655

symmetry

MDPI

Article

Circuit Complexity in Interacting Quenched Quantum Field Theory

Sayantan Choudhury [1,*], Rakshit Mandish Gharat [2], Saptarshi Mandal [3] and Nilesh Pandey [4]

[1] Centre For Cosmology and Science Popularization (CCSP), SGT University, Gurugram 122505, India
[2] Department of Physics, National Institute of Technology Karnataka, Surathkal 575025, India
[3] Department of Physics, Indian Institute of Technology Kharagpur, Kharagpur 721302, India
[4] Department of Applied Physics, Delhi Technological University, Delhi 110042, India
* Correspondence: sayantan_ccsp@sgtuniversity.org or sayanphysicsisi@gmail.com

Abstract: In this work, we explore the effects of quantum quenching on the circuit complexity of quenched quantum field theory with weakly coupled quartic interactions. We use the invariant operator method under a perturbative framework to compute the ground state of this system. We give the analytical expressions for specific reference and target states using the ground state of the system. Using a particular cost functional, we show the analytical computation of circuit complexity for the quenched and interacting field theory. Furthermore, we give a numerical estimate of circuit complexity with respect to the quench rate, δt, for two coupled oscillators. The parametric variation in the unambiguous contribution of the circuit complexity for an arbitrary number of oscillators has been studied with respect to the dimensionless parameter $(t/\delta t)$. We comment on the variation in the circuit complexity for different values of coupling strength, different numbers of oscillators and even in different dimensions.

Keywords: quantum circuit complexity; quantum quench; lattice quantum field theory

check for updates

Citation: Choudhury, S.; Gharat, R.M.; Mandal, S.; Pandey, N. Circuit Complexity in Interacting Quenched Quantum Field Theory. *Symmetry* **2023**, *15*, 655. https://doi.org/10.3390/sym15030655

Academic Editor: Valeriy Sbitnev

Received: 7 February 2023
Revised: 23 February 2023
Accepted: 3 March 2023
Published: 5 March 2023

1. Introduction

The quest to understand the fundamental laws of nature has driven research in both high energy physics and quantum information theory, leading to a remarkable interplay between these fields. By applying information-theoretic tools to the study of various quantum systems, researchers have made groundbreaking discoveries, revealing the deep connections between seemingly disparate areas of physics [1–7]. As we continue to explore the interconnections between these fields, we can look forward to new insights and discoveries that have the potential to transform our understanding of the universe.

Circuit complexity is a fundamental concept in quantum information theory that studies the computational resources required to solve a problem using quantum circuits. Formally, circuit complexity measures the minimum number of gates required to implement a given quantum computation as a function of the size of the input. The study of circuit complexity plays a crucial role in designing efficient quantum algorithms and understanding the power and limitations of quantum computers.

Since Leonard Susskind and their collaborators proposed the use of circuit complexity to study the interior of black holes [8–15], this approach has been extended to the study of quantum field theories. Researchers have found that circuit complexity can provide a useful tool for characterizing the complexity of entangled states in these theories and understanding their dynamics [16–19].

In the realm of many-body physics, the study of quantum quenches has become increasingly important in recent years, as it offers a powerful way to drive systems out of equilibrium and explore their dynamics [20–22]. In a quantum quench, a time-dependent parameter is suddenly or slowly varied, driving the system away from its ground state and potentially leading to thermalization. The study of entanglement in the context of

quenched systems has been a key area of investigation [23–32]. Moreover, the measurement of circuit complexity in quenched systems has emerged as a valuable tool for quantifying the computational resources required to simulate their dynamics [33,34]. Together, these studies shed light on the fundamental principles of non-equilibrium dynamics in quantum systems, and may pave the way for the development of novel quantum technologies.

In dynamical systems, the time-dependent Schrödinger equation plays a crucial role in understanding their evolution over time. To tackle this problem, the Lewis–Resenfeld invariant operator method has been developed, which allows one to determine the time-dependent eigenstates of such systems [35]. Additionally, the method can be extended to consider the adiabatic evolution of time-dependent parameters [36,37], providing a means to compute time-independent perturbative corrections to the eigenstates [38]. The exact form of time-dependent parameters in these eigenstates can be found by solving the Ermakov–Milne–Pinney equation, which can be efficiently computed using the Mathematica software. These methods offer a powerful means to investigate the behavior of dynamical systems, shedding new light on the intricate interplay between their time-dependent parameters and their evolution over time.

In this research article, we investigate the circuit complexity of an interacting (quartic) quenched quantum field theory using the invariant operator method as described in the appendix of our previous work [39]. The quench protocol we employ is the most commonly studied in the literature, and we use the results of [19] based on Nielsen's geometric approach to compute the circuit complexity. Specifically, we focus on graphically representing the time evolution of the unambiguous contribution of circuit complexity under different parametric variations. Our findings contribute to the growing body of literature on circuit complexity in quantum field theory and provide insights into the dynamics of complex interacting systems. For more details on the chosen quench protocol and methodology, readers can refer to [19,33,40].

The organization of the paper is as follows:

- Discretising quantum field theory (QFT) with quartic interaction on a lattice, we decouple the Hamiltonian using Fourier modes in Section 2. Evidently, the decoupled Hamiltonian refers to that of N coupled oscillators having a quartic perturbative coupling. The frequency of these oscillators is quenched by choosing a particular protocol.
- In Section 3, we use the invariant operator method to compute the time-dependent ground states and also the first-order perturbative corrections to the ground state of the quenched Hamiltonian. Notably, our research article represents the first time that this method has been applied to the computation of circuit complexity in quenched field theory. This innovative approach allows for a more comprehensive understanding of the dynamics of complex interacting systems and provides new insights into the behavior of circuit complexity under quenched conditions.
- Using the ground, we fix a specific reference and target state in Section 4. We then evaluate the circuit complexity of the chosen reference and target state in interacting (quartic) quenched quantum field theory using a particular cost function. We also evaluate the continuum limit of circuit complexity. Our results are based on a modification of the results presented in [19], which is founded on Nielsen's geometric approach [41–44]. The method we use is more general than the covariance matrix approach used in [33] and is, therefore, applicable in a perturbative framework.
- In Section 5, we numerically evaluate circuit complexity for different sets of parameters and comment on the dynamical behavior of the circuit complexity in three different regimes.
- Section 6 encapsulates the conclusions we draw from the results obtained in this work.

2. The Setup and the Quench Protocol

While the effect of quenching on free field theories has been previously studied, this is one of the first attempts to understand its impact in the context of interacting theory. To begin, we focus on a scalar field theory with the $\hat{\lambda}\phi^4$ interaction term, which we regulate by

placing it on a lattice. Once discretized, the Hamiltonian represents a family of N coupled anharmonic oscillators. We transform the original coordinates to normal modes to decouple the Hamiltonian, which allows us to compute the eigenstates for the system in a simpler way. To facilitate comparison with previous works, we follow the notations used in [16,19]. We also describe the time-dependent quench profile chosen, which is the frequency of these oscillators. The Hamiltonian for scalar field theory with a $\hat{\lambda}\phi^4$ interaction is given by [16],

$$\mathcal{H} = \frac{1}{2}\int d^{d-1}x \left[\pi(x)^2 + (\nabla\phi(x))^2 + m^2\phi(x)^2 + \frac{\hat{\lambda}}{12}\phi(x)^4\right], \tag{1}$$

where d contains the space-time dimensions. We assume the coupling $\hat{\lambda} << 1$, so that we can work in a perturbative framework. This theory can be discretized on a $d-1$ dimensional lattice, which is characterized by a lattice spacing δ.

Closely following the prescription shown in [16,19] by making proper substitutions one can show that the Hamiltonian for scalar field theory having quartic interaction term can be expressed as,

$$\mathcal{H} = \sum_{\vec{n}}\left\{\frac{\hat{P}(\vec{n})^2}{2M} + \frac{1}{2}M\left[\omega^2\hat{X}(\vec{n})^2 + \eta^2\sum_i\left(\hat{X}(\vec{n}) - \hat{X}(\vec{n}-\hat{x}_i)\right)^2 + 2\lambda\hat{X}(\vec{n})^4\right]\right\}, \tag{2}$$

where $\vec{n}$ denotes the spatial location of the points on the lattice, $\hat{x}_i$ represents the unit vectors along the lattice, ω represents the frequency of individual oscillators and η denotes inter-mass coupling. The above Hamiltonian in Equation (2) represents a family of infinitely coupled anharmonic oscillators. We use normal mode coordinates as a discrete Fourier transform of the original coordinates, given by:

$$x_a = \frac{1}{\sqrt{N}}\sum_{k=0}^{N-1}\exp\left[i\frac{2\pi a}{N}k\right]\tilde{x}_k \tag{3}$$

$$p_a = \frac{1}{\sqrt{N}}\sum_{k=0}^{N-1}\exp\left[i\frac{2\pi a}{N}k\right]\tilde{p}_k \tag{4}$$

Setting $M = 1$ for simplicity, the Hamiltonian of Equation (2) can be rewritten in normal modes as:

$$H = H_k + H'_{\phi^4}\ , \tag{5}$$

where

$$H_k = \frac{1}{2}\sum_{k=0}^{N-1}\left[|\tilde{p}_k|^2 + \omega_k^2|\tilde{x}_k|^2\right] \tag{6}$$

denotes the unperturbed (free) Hamiltonian which can be decoupled for each of the N oscillators. Here,

$$\omega_k^2 = \omega^2 + 4\eta^2\sin^2\left(\frac{\pi k}{N}\right) \tag{7}$$

denotes the frequency for each of the N oscillators. The exact form of the eigenstates for the unperturbed Hamiltonian of Equation (6) has been computed in Section 3.1.

On the other hand, the $\lambda\phi^4$ perturbation term in the Hamiltonian of Equation (5) can be dealt with by transforming the form of perturbations in normal modes:

$$\begin{aligned} H'_{\phi^4} &= \frac{\lambda}{N}\sum_{k_1,k_2,k_3=0}^{N-1}\tilde{x}_\alpha\tilde{x}_{k_1}\tilde{x}_{k_2}\tilde{x}_{k_3}\ ; \\ \alpha &= N - k_1 - k_2 - k_3 \bmod N \end{aligned} \tag{8}$$

The contribution of the above Hamiltonian in Equation (8) is evaluated by approximating the first-order correction to the eigenstates of the unperturbed Hamiltonian by employing the use of time-independent perturbation theory in Section 3.2.

We now consider the frequency, ω, in Equation (7) as a time-dependent quench profile. One of the most common quench profiles used in the literature [40] is given by:

$$\omega^2(t/\delta t) = \omega_0^2\left[\tanh^2\left(\frac{t}{\delta t}\right)\right], \tag{9}$$

where ω_0 can be considered as a free parameter and δt measures the quench rate. We choose this particular quench profile since it admits an exact solution for the mode functions given in [40]. Note that this profile attains a constant value at very early and late time. Furthermore, for this chosen form of quench profile, dynamical changes in the system occur in the time window $[-\delta t, \delta t]$. We will set $t/\delta t = T$ and $\omega_0 = 1$. The respective frequencies in the normal mode basis take the following form,

$$\omega_k = \sqrt{\omega(T)^2 + 4\eta^2 \sin^2\left(\frac{\pi k}{N}\right)}, \tag{10}$$

where $\omega(T)$ is the quench profile in Equation (9) and k runs from 0 to $N-1$.

As the frequency of each oscillator now depends on time, the unperturbed Hamiltonian is evidently time-dependent. We employ the use of the invariant operator method to compute the exact form of the unperturbed Hamiltonian. We emphasize that the perturbed Hamiltonian is not time-dependent and hence can be used as a time-independent perturbation applied to N coupled oscillators. Using the ground state of the total Hamiltonian of Equation (5), we construct the reference as well as target states, which are further used to evaluate the circuit complexity of this interacting quench model.

3. Constructing a Wave Function for a ϕ^4 Quench Model

In this section, our prime objective is to derive an analytical expression for the eigenstates of the Hamiltonian in Equation (5) by using the Lewis–Resenfield invariant operator method and approximate it to the first-order perturbative correction. The expression for eigenstates of the decoupled and unperturbed Hamiltonian in Equation (6) is derived using the invariant operator method in Section 3.1. The first order perurbative correction to the ground state of the decoupled Hamiltonian is derived in Section 3.2.

3.1. Eigenstates and Eigenvalues for Unperturbed Hamiltonian

As shown earlier, in the normal mode basis, the unperturbed Hamiltonian of Equation (6) for N oscillators is decoupled. The wavefunction for any generic state of the N oscillators is then a product of the eigenstates for each decoupled Hamiltonian of Equation (6):

$$\psi_{n_0\cdots n_{N-1}}(\tilde{x}_0, \cdots \tilde{x}_{N-1}, T) = \psi_{n_0}(\tilde{x}_0, T)\psi_{n_1}(\tilde{x}_1, T)\cdots\psi_{n_{N-1}}(\tilde{x}_{N-1}, T). \tag{11}$$

where T denotes the time dependence of the eigenstates, emerging due to the quenched frequency in Equation (9). We deal with these time-dependent eigenstates by employing the use of the invariant operator method, closely following the method of [45]. In Appendix A, we have briefly mentioned the steps one can follow to compute an analytical expression for the eigenstates of a quenched Hamiltonian of Equation (6) using the invariant operator method. Using Equation (A11) and the arguments given in Appendix A, one can show that the expression for the eigenstate of the total unperturbed Hamiltonian of N coupled oscillators is:

$$\psi^{(0)}_{n_1\cdots n_{N-1}} = \left(\frac{1}{2^{n_0+n_1+\cdots+n_{N-1}}n_0!\cdots n_{N-1}!}\right)\left(\frac{g_0g_1\cdots g_{N-1}}{\pi^N}\right)^{1/4}\exp\left[-\frac{i}{2}\sum_{k=0}^{N-1}(2n_k+1)\gamma_k\right]\exp\left[-\frac{1}{2}\sum_{k=0}^{N-1}\tilde{v}_k\tilde{x}_k^2\right] \times \mathbf{H}_{n_0}\left[\sqrt{\dot{\gamma}_0}\tilde{x}_0\right]\cdots\mathbf{H}_{n_{N-1}}\left[\sqrt{\dot{\gamma}_{N-1}}\tilde{x}_{N-1}\right] \tag{12}$$

where $g_k = \dot{\gamma}_k$ and

$$\tilde{v}_k = \dot{\gamma}_k\left(1 - \frac{i\dot{\rho}_k}{\rho_k\dot{\gamma}_k}\right) \tag{13}$$

for $k = 0, 1\cdots, N-1$. All other symbols used in Equation (12) are defined in Appendix A. In this work, we focus on the ground state of the wavefunction shown in Equation (12), which can be written as:

$$\psi^{(0)}_{0\cdots 0} = \left(\frac{g_0g_1\cdots g_{N-1}}{\pi^N}\right)^{1/4}\exp\left[-\frac{1}{2}\sum_{k=0}^{N-1}(i\gamma_k + \tilde{v}_k\tilde{x}_k^2)\right]. \tag{14}$$

To compute the eigenvalues of the unperturbed quenched Hamiltonian in Equation (6), one can again use the invariant operator method. From the arguments given in [38], the energy eigenvalues for time-dependent harmonic oscillators can be evaluated by multiplying the time-dependent factor by the expression of the energy eigenvalues of time-independent harmonic oscillators. Hence, one can show that the energy eigenvalues for each of the N decoupled oscillators become:

$$\langle\psi_{n_k}|\, H_i\,|\psi_{n_k}\rangle = W_k(T)\left[n_k + \frac{1}{2}\right], \tag{15}$$

where $W_k(T)$ for $k = 0, \cdots, N-1$ is a time-dependent factor for each oscillator given by,

$$W_k(T) = \frac{\dot{\gamma}_k}{2}\left(\frac{\dot{\rho}_k + \rho_i^2\rho_i^2 + \rho_i^2\dot{\gamma}_i}{\rho_i^2\dot{\gamma}_i{}^2}\right). \tag{16}$$

Using the above form of time-dependent eigenvalues, one can compute the energy eigenvalues for the decoupled Hamiltonian of Equation (6), which is given by:

$$\langle\psi^{(0)}_{n_1,\cdots,n_{N-1}}|\, H\,|\psi^{(0)}_{n_1,\cdots,n_{N-1}}\rangle = \sum_{k=0}^{N-1} W_k\left(n_k + \frac{1}{2}\right). \tag{17}$$

The above expression for the eigenvalues of the unperturbed Hamiltonian can now be used to approximate the first order time-independent perturbative correction to the ground state of Equation (14).

3.2. Wavefunction for $\lambda\phi^4$ Perturbation Applied to the Ground State of N Quenched-Coupled Oscillators

In this section, our prime objective is to evaluate the analytical expression for the wavefunction of the ground state of N coupled oscillators in a perturbative framework, approximated to first order. We consider $\psi^{(1)}$ to be the first-order correction arising due to the Hamiltonian in Equation (8). Hence, using Equation (14), the expression for the ground state of the total Hamiltonian (Equation (5)) corrected to first order in λ can be written as:

$$\psi_{0,0,\cdots 0}(\bar{x}_0,\cdots\tilde{x}_{N-1}) = \left(\frac{g_0g_1\cdots g_{N-1}}{\pi^N}\right)^{1/4}\times\exp\left[-\frac{1}{2}\sum_{k=0}^{N-1}(i\gamma_k + \tilde{v}_k\tilde{x}_k^2 + \lambda\psi^1)\right]. \tag{18}$$

We take note of the fact that for N coupled oscillators, the $\lambda\phi^4$ perturbation can give rise to a combination of five terms, viz., $x_a^4, x_b^2x_c^2, x_dx_e^3, x_fx_g^2x_h$ and $x_ix_jx_kx_l$. Hence, we have expressed the form of the first-order correction by closely following the notations used in [19],

$$\psi_4^1 = \sum_{\substack{a=0 \\ 4a \bmod N \equiv 0}}^{N-1} B_1(a) + \sum_{\substack{b,c=0 \\ (2b+2c) \bmod N \equiv 0 \\ b \neq c}}^{N-1} \frac{B_2(b,c)}{2} + \sum_{\substack{d,e=0 \\ (3e+d) \bmod N \equiv 0 \\ d \neq e}}^{N-1} B_3(d,e) + \sum_{\substack{f,m,h=0 \\ (f+2m+h) \bmod N \equiv 0 \\ f \neq m \neq h}}^{N-1} \frac{B_4(f,m,h)}{2} + \sum_{\substack{i,j,k,l=0 \\ (i+j+k+l) \bmod N \equiv 0 \\ i \neq j \neq k \neq l}}^{N-1} \frac{B_5(i,j,k,l)}{24}. \tag{19}$$

One can compute the exact form of coefficients for each of the five different perturbative terms by first choosing an appropriate number of oscillators and then generalizing the result for N oscillators. Furthermore, one can compute the perturbative correction by setting V as each perturbative term mentioned above, and then using the formula given below,

$$\psi^{(1)}_{0,\cdots 0} = \sum_{(n_0 \cdots n_{N-1}) \neq (0,\cdots 0)} \frac{\langle \psi^{(0)}_{n_0,\cdots n_{N-1}} | \, V \, | \psi^{(0)}_{0,\cdots 0} \rangle \times \psi^{(0)}_{n_0,\cdots n_{N-1}}}{\langle \psi^{(0)}_{0,\cdots 0} | \, H \, | \psi^{(0)}_{0,\cdots 0} \rangle - \langle \psi^{(0)}_{n_0,\cdots n_{N-1}} | \, H \, | \psi^{(0)}_{n_0,\cdots n_{N-1}} \rangle}. \tag{20}$$

For example, if one wants to obtain the form of $B_3(d,e)$ in Equation (19), set the number of oscillators to $N = 2$ and put $V = x_0x_1^3$ into Equation (20). The form of the perturbative expansion thus obtained can be generalized for an arbitrary number of N oscillators. We then repeat these steps to fix all the coefficients of perturbative expansion. The exact form of all these coefficients, using Equation (20), is tabulated in Appendix D.

4. Analytical Calculation for Circuit Complexity of ϕ^4 Quench Model

The ground state of the total Hamiltonian, calculated in the previous section and given by Equation (18), is used to construct the reference and target states in Section 4.1. Choosing a specific cost functional, we have derived the analytical expression for circuit complexity by modifying the results of [19] in Section 4.2.

4.1. Constructing Target/Reference States

In the wavefunction for N oscillators with quartic perturbation shown in Equation (18), following the method given in [19] one can write the exponent in the form of a matrix conjugated by a basis vector $\vec{v}$. The wavefunction then takes the below given form:

$$\psi^s_{0,0,\cdots 0}(\tilde{x}_0, \cdots, \tilde{x}_{N-1}) \approx \mathcal{N}^s \exp\left[-\frac{1}{2} v_a A^s_{ab} v_b\right] \tag{21}$$

where $\mathcal{N}^s$ denotes the normalization factor and A^s denotes a block diagonal matrix for the respective state. Furthermore, the space of circuits is parameterized by setting value of the running parameter s. At $s = 1$, the above form of the wavefunction coincides with the wavefunction in Equation (18), such that $\mathcal{N}_{s=1}$ becomes the normalizing factor of Equation (18) by an appropriate choice of the basis $\vec{v}$. Then, $\psi^{s=1}_{0,0,\cdots 0}$ is referred to as the target state. There are many possible choices for choosing bases so as to obtain the terms in the perturbative expansion in Equation (19). However, as a minimal choice we choose the below mentioned basis,

$$\vec{v} = \{\tilde{x}_0, \cdots \tilde{x}_{N-1}, \tilde{x}_0^2, \cdots, \tilde{x}_{N-1}^2, \cdots, \tilde{x}_a\tilde{x}_b, \cdots\}. \tag{22}$$

In this basis, one can show that the matrix A in Equation (21) has a block diagonal form:

$$A_{ab}^{s=1} = \begin{pmatrix} A_1 & 0 \\ 0 & A_2 \end{pmatrix}. \tag{23}$$

A_1 contains coefficients of terms such as x_a^2 and $x_a x_b$ in Equation (18) multiplied by -2. All the elements of A_1 can be fixed to obtain a specific form of target state. This block is often referred to as the *unambiguous* block.

The elements of the A_2 block consist of coefficients which are basis dependent, i.e., there is not a unique choice of basis vector for defining the elements of the A_2 block because, unlike the A_1 block which only consists of coefficients of quadratic terms which can be defined uniquely without any ambiguity, the A_2 block consists of elements which are coefficients of terms such as $\tilde{x}_a^2\tilde{x}_b^2$, $\tilde{x}_a^2\tilde{x}_b^2\tilde{x}_c^2$ and $\tilde{x}_a\tilde{x}_b\tilde{x}_c\tilde{x}_d$, which can be defined in several ways. Due to this arbitrariness, the complexity for the ambiguous block will be different for different choices of basis. One cannot therefore fix elements of A_2 such that the contribution of A_2 to the total complexity of the system is independent of the choice of basis. Due to these ambiguities, the A_2 block is often referred to as the *ambiguous* block. We construct the reference state by choosing the value of all the frequencies for each of the N oscillators as $\tilde{\omega}_{ref}$. Since all the oscillators have the same frequency, the reference state evidently would be time independent. Then, the wavefunction in Equation (19) can be modified to that of reference state mentioned below,

$$\psi^{s=0}(x_1, x_2, ..., x_n) = \mathcal{N}^{s=0} \exp\Big[-\sum_{i=0}^{N-1} \frac{\tilde{\omega}_{ref}}{2}\big(x_i^2 + \lambda^0 x_i^4\big)\Big]. \tag{24}$$

Note that λ^0 is a parameter denoting the non-Gaussian nature of the reference state and is not to be confused with the perturbative coupling λ used in the target state. In normal modes, the above expression can be recast as shown below,

$$\psi^{s=0}(\tilde{x}_1, \tilde{x}_2, ..., \tilde{x}_n) = \mathcal{N}^{s=0} \exp\Big[-\frac{1}{2}\Big(v_a A_{ab}^{s=0} v_b\Big)\Big], \tag{25}$$

where the matrix $A_{ab}^{s=0}$ can be fixed as:

$$A_{ab}^{s=0} = \begin{pmatrix} \tilde{\omega}_{ref}\mathbb{I}_{N\times N} & 0 \\ 0 & A_2^{s=0} \end{pmatrix}. \tag{26}$$

Again, there will be ambiguities in fixing the elements of $A_2^{s=0}$ for the reasons already mentioned above.

Equipped with the target and and reference states for the quenched and interacting oscillators, we can proceed to give an analytical expression for circuit complexity by getting around the ambiguities in the upcoming subsection.

4.2. Analytical Calculation of the Complexity Functional

In this subsection, we outline the analytical steps to compute the expression for circuit complexity for the previously mentioned target state (Equation (18)) starting with a reference state (Equation (25)) using the results of [19].

As shown in [33], the complexity functional depends on the chosen cost function. In this article, we work with the following cost function,

$$\mathcal{F}_\kappa(s) = \sum_I p_I |Y^I|^\kappa. \tag{27}$$

As shown in [19,46], the circuit complexity with this particular cost function becomes,

$$\mathcal{C}_\kappa = \int_{s=0}^{1} \mathcal{F}_\kappa \, ds. \tag{28}$$

Next, we write the complexity as the sum of two terms,

$$\mathcal{C}_\kappa = \mathcal{C}_\kappa^{(1)} + \mathcal{C}_\kappa^{(2)}, \tag{29}$$

where $\mathcal{C}_\kappa^{(1)}$ refers to the contribution to the circuit complexity from A_1 block while $\mathcal{C}_\kappa^{(2)}$ refers to the contribution from A_2 block. $\mathcal{C}_\kappa^{(1)}$ and $\mathcal{C}_\kappa^{(2)}$ can be given as the ratio of eigenvalues of the respective blocks for the chosen target (18) and reference states (Equation (25)) as demonstrated in [19,33],

$$\mathcal{C}_\kappa = \frac{1}{2^\kappa} \sum_{i=0}^{N-1} \left| log\Big(\frac{\Lambda_i^{(1)}}{\tilde{\omega}_{ref}}\Big)\right|^\kappa + \mathcal{A} \sum_j \left| log\Big(\frac{\Lambda_j^{(2)}}{h_i \tilde{\omega}_{ref} \lambda_0}\Big)\right|^\kappa, \tag{30}$$

where $\mathcal{A}$ denotes the penalty factor. Due to the ambiguities arising while fixing the form of the A_2 block, numerically one cannot fix the form of $\Lambda_i^{(2)}$. However, as discussed in Appendix C, we can choose a minimal basis such that the elements of A_2 are fixed for $N = 2$ oscillators. In Appendix C, we have computed the total circuit complexity for $N = 2$ coupled oscillators with a quenched Hamiltonian with quartic coupling.

In this work, have neglected the contribution of the ambiguous block, i.e., $\mathcal{C}_\kappa^{(2)}$, as we cannot find any basis to determine the numerically exact contribution of the A_2 block for an arbitrary number of oscillators. Nonetheless, we attempt to give an analytical form of $\mathcal{C}_{\kappa=1}^{(2)}$ in terms of renormalized parameters in Appendix B, again following the steps shown in [19].

4.3. The Continuum Limit for $\mathcal{C}_1$

Now, we will compute the exact form of the eigenvalues of the A_1 block taking the continuum limit. To find the form of $\Lambda_i^{(1)}$, we now reinstate the factor M, previously set to $M = 1$ in Section 2. In light of this, the Hamiltonian given in Equation (5) will change, although it will retain the previous form of eigenvalues and eigenfunctions. The new Hamiltonian with a factor of M becomes,

$$H = \frac{1}{M} \sum_{\vec{n}} \Big\{ \frac{P(\vec{n})^2}{2} + \frac{1}{2} M^2 \Big[\omega^2 X(\vec{n})^2 + \Omega^2 \sum_i (X(\vec{n}) - X(\vec{n} - \hat{x}_i))^2 + 2\{\lambda_4 X(\vec{n})^4\} \Big] \Big\}. \tag{31}$$

Considering the reinstated factor of M, we rescale some of the parameters as shown below,

$$\omega \to \frac{\omega}{\delta}; \quad \eta \to \frac{\eta}{\delta}; \quad \lambda \to \frac{\lambda}{\delta^2}; \quad \tilde{\omega}_{ref} \to \frac{\tilde{\omega}_{ref}}{\delta}; \quad \lambda^0 \to \frac{\lambda^0}{\delta}.$$

Using these rescaled parameters, one can generalize the form of eigenvalues $\Lambda_i^{(1)}$ using Mathematica by considering trial cases for different values of N and eliminating all the factors, except for ρ_k and $\tilde{\omega}_k$, by using the appropriate formulae mentioned in previous sections. Below, we show the generalized formula for the eigenvalues of the $A_1^{(s=1)}$ block depending on whether the chosen number of oscillators, N, is even or odd,

$$\begin{aligned} \Lambda_i &= \frac{3\lambda\rho_i^2}{2N} \left(\frac{g_\alpha + 2g_i}{g_\alpha(\rho_i^2(g_i + \omega_i^2) + \dot{\rho}_i)} - \frac{2g_i\rho_\alpha^2}{\rho_i^2(\rho_\alpha^2(\omega_i^2 g_\alpha + g_i(2g_\alpha + \omega_\alpha^2)) + g_i\dot{\rho}_\alpha) + \dot{\rho}_i g_\alpha \rho_\alpha^2} \right) + \frac{\tilde{v}_i}{2}, \quad N\text{: Even} \\ &= \frac{3\lambda g_i^2 \rho_i^4 \left((g_i + \omega_i^2)\rho_i^2 + \dot{\rho}_i\right)}{N g_i (\rho_i^2(g_i + \omega_i^2) + \dot{\rho}_i)\left(\rho_i^2(\rho_i^2(g_i\omega_i^2 + g_i(2g_i + \omega_i^2)) + g_i\dot{\rho}_i) + g_i\dot{\rho}_i\rho_i^2\right)} + \frac{\tilde{v}_i}{2}, \quad N\text{: Odd} \end{aligned} \tag{32}$$

where the index $\alpha = |N/2 - i|$. One can insert this expression for the eigenvalues into Equation (30) to obtain the desired value of circuit complexity. We emphasize that the form of these eigenvalues makes the circuit complexity a time-dependent quantity due to the chosen quench profile. This time-dependence of the complexity is explored in numerical plots by choosing an appropriate time scale.

One can check the behavior of circuit complexity, C_1, at the continuum limit: $N \to \infty$ while $\delta \to 0$ such that $L = (N\delta)$ is finite.

Now, in arbitrary dimensions, the equation for $\mathcal{C}^{(1)}_{\kappa=1}$ can be rewritten as:

$$\mathcal{C}^{(1)}_{\kappa=1} = \frac{1}{2}\sum_{k=1}^{d-1}\sum_{i=0}^{N-1}\left|log\left(\frac{\Lambda^{(1)}_i}{\tilde{\omega}_{ref}}\right)\right|. \tag{33}$$

For simplicity, if one chooses to set the same frequency (of the respective oscillator) in each dimension, d, then one can write:

$$\omega_i = \sqrt{\frac{1}{d-1}\left[4(d-1)\eta^2\sin^2\left(\frac{\pi i}{N}\right) + \omega_0^2\tanh^2\left(\frac{t}{\delta t}\right)\right]}. \tag{34}$$

Hence, in arbitrary dimensions d, the circuit complexity can be still be computed using Equation (30), thus getting rid of the lattice sums in Equation (33) such that the frequencies are set by Equation (34).

5. Numerical Results

In this section, we numerically evaluate the value of circuit complexity for coupled oscillators using the expressions computed for the total complexity of two coupled oscillators, denoted by $\mathcal{C}$ and shown in Appendix C, and the unambiguous contribution of the complexity on the arbitrary number of oscillators using the results of Section 4.3, henceforth denoted by $\mathcal{C}_1$. We will use a finite lattice for our numerical evaluation and will discretize the time steps to plot the behavior of the obtained circuit complexity. Note that each time-dependent coefficient in these expressions explicitly depends on $\rho_k(t, \delta t)$ given by Equation (A7). To obtain the values of A, B and C which can be inserted into Equation (A7), we set some straightforward initial conditions. The invariant quantities, Ω_k in Equation (A8), are taken to be $\Omega_k = 1$. Using the values of $\rho_k(t, \delta t)$ for $t \to 0$, we obtain the desired values of A, B and C by setting $\rho_k(0, \delta t) = 1$ and $\gamma_k(0, \delta t) = 0$ by using $AC - B^2 = \Omega^2$. The coupling between the oscillators is set to $\eta = 0.25$. The free parameter in the quench profile, Equation (9), is set to $\omega_0 = 1$. The frequency of the reference state is set to $\omega_{ref} = 0.001$.

Using the exact values of circuit complexity, we parameterize four different plots in this section. The first plot features the behavior of the total complexity, $\mathcal{C}$, computed for two coupled oscillators discretized on a lattice of size $L = 20$, varying with the quench rate, δt. This plot is divided into two regions, $\delta t < 1$ is the sudden quench limit (blue) region, while $\delta t > 1$ is the slow quench limit (yellow) region. The next three plots characterize the behavior of the unambiguous contribution of the circuit complexity, C_1, for more than two coupled oscillators discretized on a lattice of size $L = 100$, varying with the dimensionless parameter $(t/\delta t)$. In these plots, we mark $(t/\delta t) = 1$ as the quench point by a dotted vertical red line. The red region for $(t/\delta t) < 1.2$ features the early time behavior of the circuit complexity, the yellow region ($0.8 < (t/\delta t) < 1.2$) shows the behavior of complexity near the quench point, while the blue region ($(t/\delta t) > 1.2$) characterizes the late time behavior of the circuit complexity.

In Figure 1, we have plotted the numerical values of total complexity for a $N = 2$ coupled oscillator system with quartic interaction using Equation (A23) with respect to the quench rate, δt. The blue colored region shows the behavior of the circuit complexity in the fast regime, $\delta << 1$. In the slow regime, initially, the circuit complexity monotonically increases until $\delta t = 0.01$. Beyond this ($\delta t = 0.01$), the complexity shows a linear scaling

with the slope, $\log \mathcal{C} / \log \delta t = 0.0825$, up to $t = 0.1$. This linear scaling is then followed by a monotonous increase in the circuit complexity until $t = 0.2$. Beyond $t = 0.2$, the circuit complexity saturates, changing the transition into a slow regime ($\delta t > 1$), marked by a yellow background. Furthermore, it is evident that, for each quartic coupling, λ, the circuit complexity shows same behavior. However, it is clear that as one increases the quartic coupling, the complexity decreases.

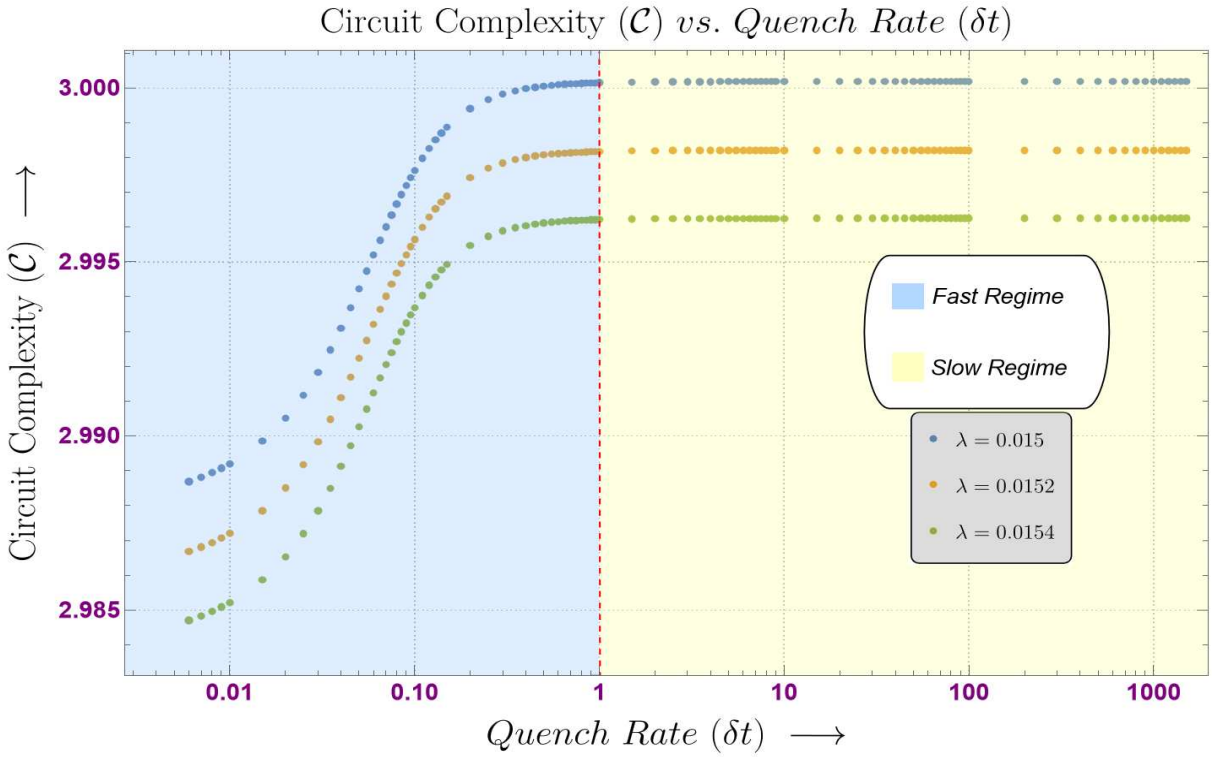

Figure 1. Log–log variation of the total circuit complexity (C) with respect to the quench rate (δt) for different orders of the coupling constant, λ, for two coupled oscillators with quartic perturbation.

Although one cannot obtain numerical results for the total circuit complexity of more than two oscillators, we have plotted the numerical values of complexity pertaining to the unambiguous block, i.e., $\mathcal{C}_1$, with respect to the dimensionless parameter $(t/\delta t)$ for $N = 10$ coupled oscillators in Figure 2. The figure is divided into three regions, the first is the early time behavior for the dimensionless parameter between $0 < (t/\delta t) < 0.8$, marked by a red background. In this region, for all the three considered quartic couplings, the circuit complexity decreases linearly up to $(t/\delta t) = 0.7$. Beyond this, for $(t/\delta t) > 0.7$, the circuit complexity, C_1, diverges for each particular quartic coupling, λ, such that the higher the value of λ, the higher the complexity, C_1. This linear scaling is then followed by a monotonous decrease in the value of C_1 as we move near the quench point, $(t/\delta t) = 1$, marked by a yellow background. The late time behavior is characterized by saturation of C_1 for $(t/\delta t) > 1.2$, which is marked by a blue background. It is evident that for different quartic couplings, λ and the circuit complexity, C_1, scale similarly in each particular region. However, as we increase the quartic coupling, λ and the circuit complexity, C_1, increase at any particular time near and beyond the quench point.

In Figure 3, we have plotted the unambiguous contribution of the circuit complexity, C_1, for discretized field theory with respect to the dimensionless parameter $(t/\delta t)$ for different numbers of oscillators, viz., $N = 10, 11$ and 12 (keeping the quartic coupling fixed at $\lambda = 0.01$). The early time behavior for a particular N is characterized by a steep linear decrease in value of the circuit complexity, C_1, up to $(t/\delta t) = 0.4$. Beyond this point, the complexity, C_1, monotonically decreases and finally saturates at $(t/\delta t) \approx 0.5$. After this point, the unambiguous contribution of the circuit complexity, C_1, remains saturated.

The early time behavior of C_1 features a decrease and a saturation in the value of complexity, marked by a red background. The behavior of C_1 near to the quench point, as well as at late time, is characterized by a constant saturated value at all times, marked by yellow and blue backgrounds, respectively. It is evident that the unambiguous contribution of circuit complexity, C_1, scales similarly for any N. However, the larger the number of oscillators, N, the larger the value of C_1. At the continuum limit, when we have large number of coupled oscillators, one can expect that the unambiguous contribution of the circuit complexity, C_1, will behave similarly to that shown in this figure.

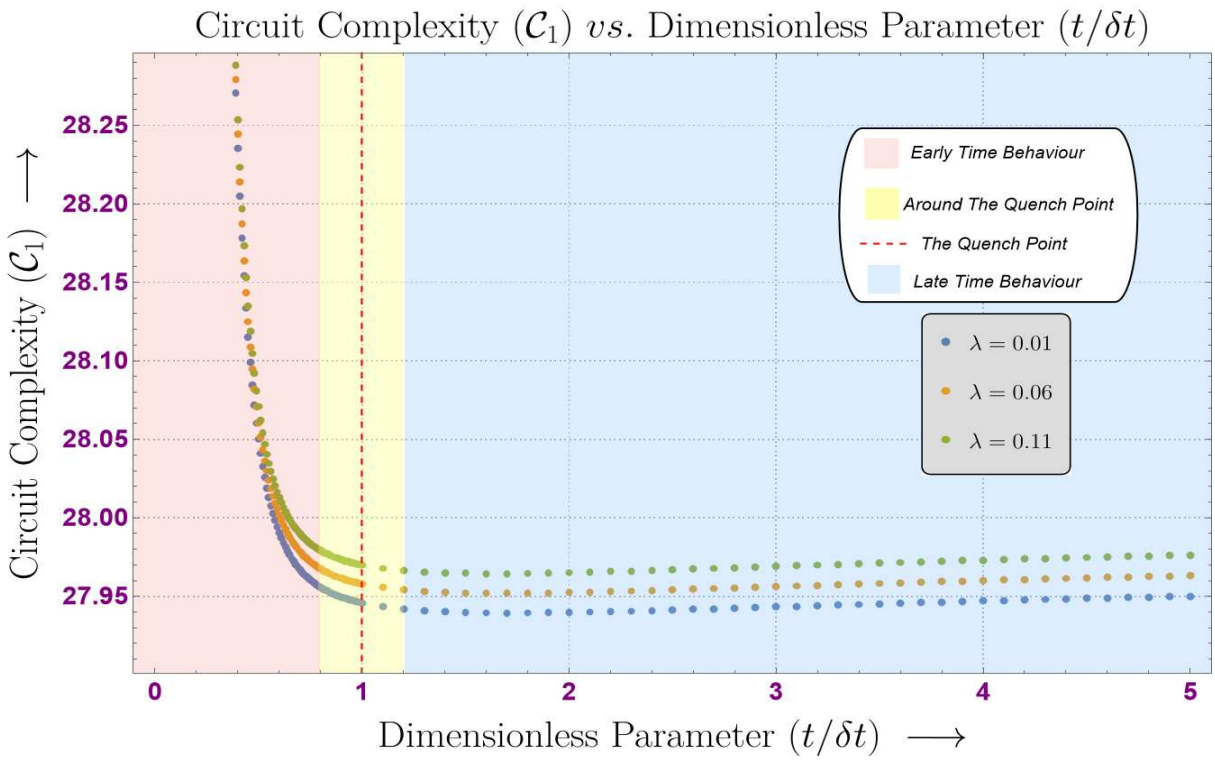

Figure 2. Variation in the circuit complexity for the A_1 block (C_1) for $N = 10$, with respect to the dimensionless parameter $(t/\delta t)$ for different orders of the coupling constant λ.

In Figure 4, we have plotted the unambiguous contribution of the circuit complexity, C_1, for discretized field theory with respect to the dimensionless parameter $(t/\delta t)$ for different numbers of dimensions, viz., $d = 2, 3$ and 4 (keeping the quartic coupling fixed at $\lambda = 0.01$ and the number of oscillators at $N = 10$). For a particular d, the early time behavior of the unambiguous contribution of the circuit complexity is characterized by a monotonous decrease in the value of C_1, marked by a red background. The values of C_1 for different dimensions, d, begin to converge near to the quench point, $(t/\delta t = 1)$, and finally saturate to a constant value, this is marked by a yellow background. At late times, the unambiguous contribution of the circuit complexity, C_1, remains saturated to a constant value, this is marked by a blue background. It is evident for any dimension d, the circuit complexity, C_1, scales similarly. However, the higher the dimension d, the larger the value of C_1 at any particular time (in the red region).

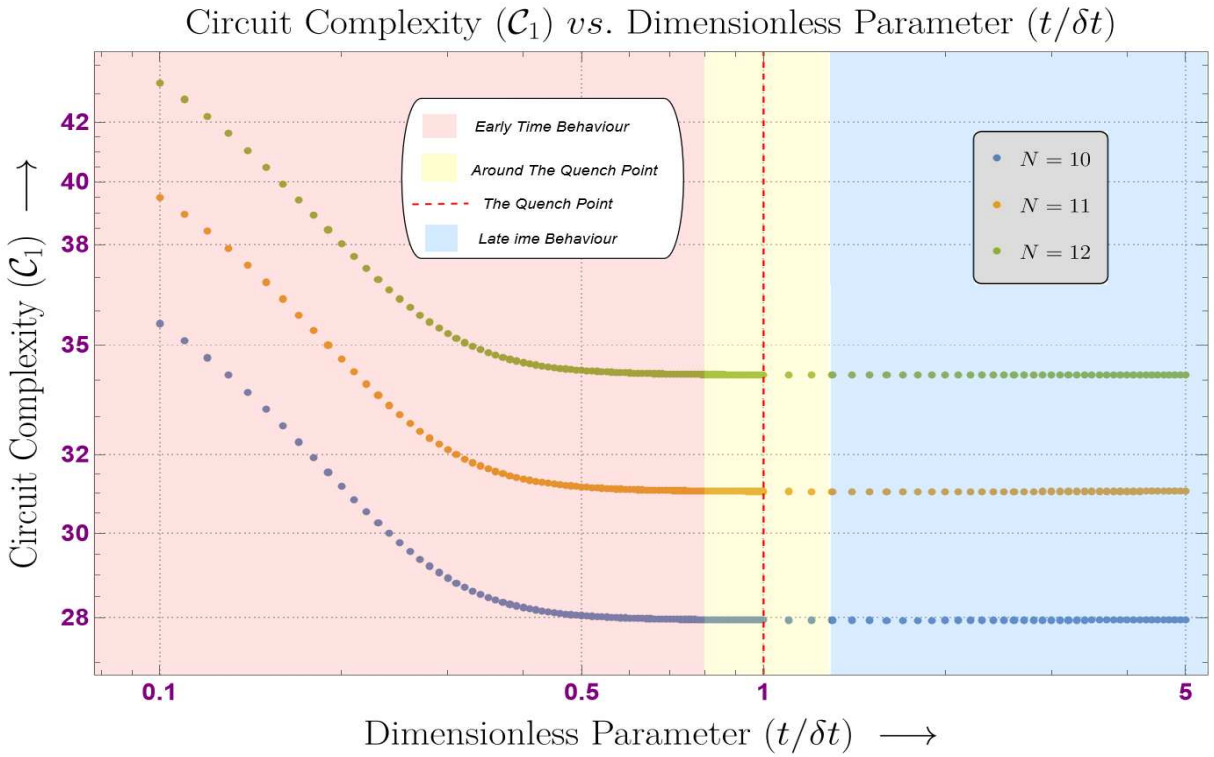

Figure 3. Semi-Log variation in the circuit complexity for the A_1 block (C_1) at $\lambda = 0.01$, with respect to the dimensionless parameter $(t/\delta t)$ for different values of N.

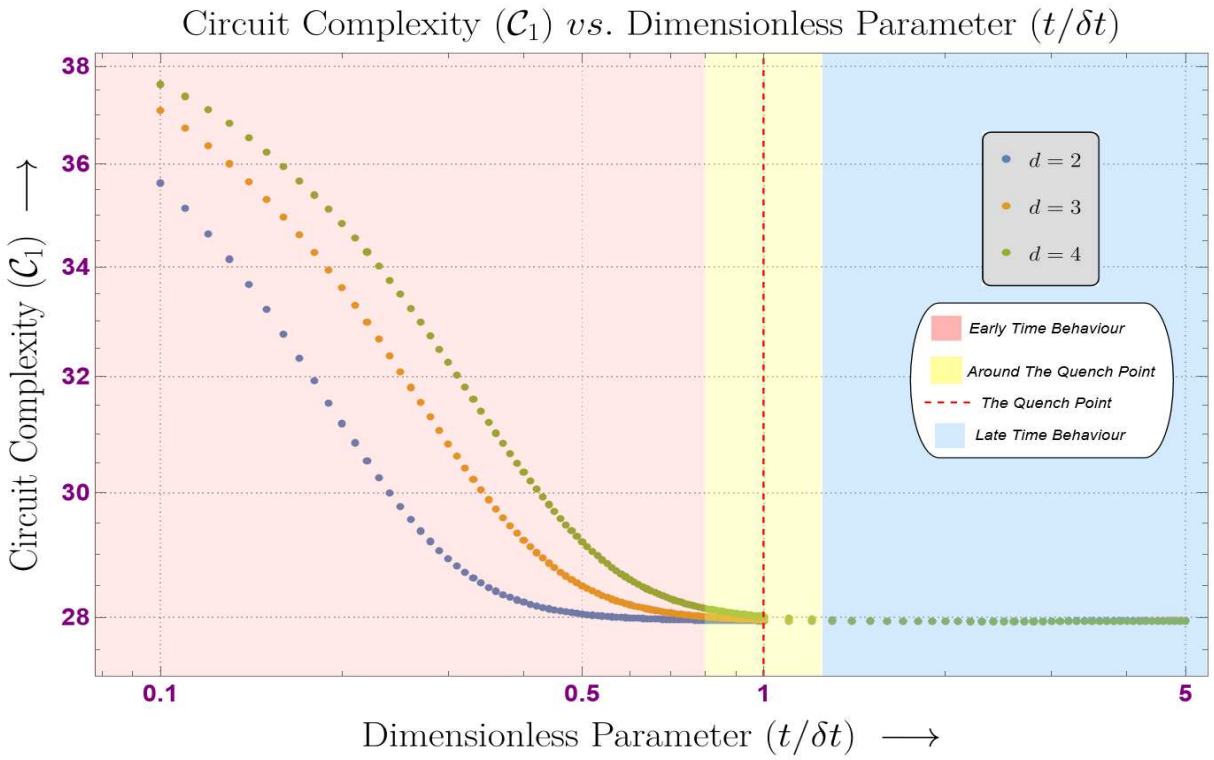

Figure 4. Semi-Log variation in the circuit complexity for the A_1 block (C_1) at $\lambda = 0.01$, $N = 10$, with respect to the dimensionless parameter $(t/\delta t)$ for different dimensions d.

6. Conclusions

In this article, we have studied the dynamic behavior of the circuit complexity in quenched field theory with quartic interactions. To do this, we have used a unique frame-

work that combines Nielsen's geometric approach based on [19,33] and the invariant operator method. While preparing the reference and target states, we have employed Nielsen's geometric approach to finding the optimal circuit out of an infinite set of circuits. This approach provided a novel perspective to understand the behavior of the complexity under different parametric conditions.

We have used the invariant operator method to find the exact form of the eigenstates of the unperturbed part of the Hamiltonian. Combining this with perturbation theory, we were able to determine approximate solutions to the time-dependent Schrödinger equation. This enabled us to derive the analytical expression for time-dependent circuit complexity using Nielsen's method.

We have discretized the field theory on a lattice and evaluated the wavefunction for N-coupled oscillators with quartic perturbation and a quenched frequency. We used the ground state wavefunction to derive the analytical form of the reference and target states. By choosing a specific cost function and a minimal basis, we computed the exact form of the total complexity for two coupled oscillators and the unambiguous contribution of circuit complexity for an arbitrary N number of oscillators. Our study thus provides a comprehensive understanding of the dynamical behavior of the circuit complexity in quenched field theory with quartic interactions.

The important results of our work are detailed below point-wise:

- For two coupled oscillators, we observed that in most parts of the sudden quench, the total circuit complexity monotonously increases at very small values of quench rate, then scales linearly and shows a trend of thermalization near $\delta t = 1$. In the slow quench limit, the complexity remains saturated irrespective of the quench rate. When parameterized for different values of quartic coupling, λ, it is evident that as the coupling increases, the circuit complexity increases.
- The exact analytical form for the unambiguous contribution of the circuit complexity for N coupled oscillators was derived using the results of [19]. The parametric variation in this circuit complexity was then plotted with respect to the dimensionless parameter $(t/\delta t)$.
- It is evident from these plots that the unambiguous contribution of the circuit complexity decreases with respect to the dimensionless parameter. When parametrized for different quartic couplings, we find that, initially, the complexity decreases linearly following the same line, irrespective of the quartic coupling. Near to the quench point, the complexity for each quartic coupling diverges and saturates at late times. After the quench point, the complexity after divergence is clearly in direct proportion to the increasing value of the quartic coupling.
- We observed that the unambiguous contribution of the circuit complexity behaves similarly, irrespective of the number of oscillators, N. However, as N increases, the respective value of the complexity increases at any particular time. Using this, we commented on the continuum limit where the results would still be the same.
- Furthermore, it is clear that the unambiguous contribution of the circuit complexity for the chosen set of parameters is proportional to the increasing number of dimensions at early times. However, at the quench point, the unambiguous contribution of the circuit complexity attains a constant value, irrespective of the number of dimensions, and thermalizes at late times.

In conclusion, we have presented a novel approach to study the time-dependent circuit complexity in the context of quenched interacting field theory. By combining the invariant operator method and Nielsen's geometric approach, we have derived the analytical expression for circuit complexity and explored its behavior under various parametric conditions. Our results demonstrate that the quenching of the system has a significant impact on the circuit complexity of interacting field theories. Our work provides a new perspective on the understanding of the dynamical behavior of circuit complexity in interacting field theories. It also opens up avenues for future research, such as the exploration of circuit complexity

in other interacting field theories and the study of its relationship with other quantum information theoretic quantities.

Future Prospects:

- In this work, we explored the effects of quantum quenching on QFT with quartic coupling. In the future, it would be interesting to explore the effects of quantum quenching on Krylov complexity [47–51] for QFT with quartic coupling.
- Some of the works focusing on understanding the connection between complexity and quantum entanglement can be found in [40,52–55]. The connection between complexity and quantum entanglement in the case of quenched theories might turn out to be fruitful.

Author Contributions: Conceptualization, S.C. ; methodology, S.C., R.M.G., S.M. and N.P.; software, R.M.G., S.M. and N.P.; validation, S.C., R.M.G., S.M. and N.P..; formal analysis, S.C., R.M.G., S.M. and N.P.; investigation, S.C.; resources, S.C., R.M.G., S.M. and N.P.; data curation, NA; writing—original draft preparation, S.C., R.M.G., S.M. and N.P.; writing—review and editing, S.C., R.M.G., S.M. and N.P..; visualization, S.C., R.M.G., S.M. and N.P.; supervision, S.C.; project administration, NA; funding acquisition, NA. All authors have read and agreed to the published version of the manuscript.

Funding: This research received no external funding.

Data Availability Statement: Not applicable.

Acknowledgments: S.C. would like to thank the work friendly environment of CCSP, SGT University for providing tremendous research support and for offering them a (Senior Grade) position. S.C. also thanks all the members of our newly formed virtual international non-profit consortium: Quantum Aspects of the Space-Time & Matter (QASTM) for elaborative discussions. R.M.G., S.M. and N.P. would like to thank the members of the QASTM Forum for useful discussions. Last but not least, we would like to acknowledge our debt to the people belonging to the various parts of the world for their generous and steady support for research in natural sciences.

Conflicts of Interest: The authors declare no conflict of interest.

Appendix A. Evaluating the Eigenstates of Unperturbed Hamiltonian Using Invariant Operator Method

In this appendix, we show the analytical steps to evaluate the expression for the eigenstates of the unperturbed Hamiltonian with a quenched (time-dependent) frequency shown in Equation (6) of Section 4. The invariant operator method is the optimal choice to compute these eigenstates as it enables one to evaluate the exact time-dependent wavefunctions by solving the time-dependent Schrodinger equation. A detailed analysis on the invariant operator method can be found in [56].

First, we define the creation $(a_k^\dagger)$ and annihilation (a_k) operators given by,

$$\begin{aligned} a_k &= \frac{1}{\sqrt{2\dot{\gamma}_k}}\left[\dot{\gamma}_k\left(1 - i\frac{\dot{\rho}_k}{\rho_k\dot{\gamma}_k}\right)\tilde{x}_k + i\tilde{p}_k\right] \\ a_k^\dagger &= \frac{1}{\sqrt{2\dot{\gamma}_k}}\left[\dot{\gamma}_k\left(1 + i\frac{\dot{\rho}_k}{\rho_k\dot{\gamma}_k}\right)\tilde{x}_k - i\tilde{p}_k\right] \end{aligned} \tag{A1}$$

where $k = 0, 1, \cdots, N-1$. Furthermore, γ_k and ρ_k are time-dependent factors while $\dot{\gamma}_k = \partial_T\gamma_k$, $\dot{\rho}_k = \partial_T\rho_k$ and $\ddot{\rho}_k = \partial_T^2\rho_k$ are not . One can show that the operators in Equation (A1) satisfy the commutation relation $[a_i, a_j^\dagger] = \delta_j^i$. We fix the time-dependent factor ρ_k as the solution to the Ermakov–Milne–Pinney equation for each oscillator,

$$\ddot{\rho}_k + \omega_k^2\rho_k = 0, \tag{A2}$$

where ω_k denotes the frequency for each coupled oscillator (Equation (10)). If we define,

$$\alpha_k = \omega_0^2 + \frac{4\eta^2\left(\sin^2\left(\frac{\pi i}{N}\right)\right)}{\tanh^2(T)}, \tag{A3}$$

for $k = 0, 1, \cdots, N-1$; then, using Equation (9), one can rewrite Equation (A2) as:

$$\ddot{\rho_k} + \alpha_k \tanh^2(T)\rho_k = 0, \tag{A4}$$

where $k = 0, 1, \cdots, N-1$. We assume that the solution to Equation (A4) is of the form:

$$\rho_k(t, \delta t) = c_1\epsilon_k^1(t, \delta t) + c_2\epsilon_k^2(t, \delta t), \tag{A5}$$

where c_1 and c_2 represent numerical constants. On the other hand, ϵ_k^1 and ϵ_k^2 are two complex valued coefficients for each $k = 0, \cdots, N-1$. However, we can consider only the term with ϵ_k^1 as one of the solutions to Equation (A4) by setting $c_2 = 0$. Using Mathematica, one can compute the exact form of ϵ_k^1, following the steps shown in [39], which are mentioned below:

$$\epsilon_k^1 = \left(e^{\frac{2t}{\delta t}}\right)^{-\frac{1}{2}i\delta t\alpha_k}\left(e^{\frac{2t}{\delta t}}+1\right)^{\frac{1}{2}\left(\sqrt{1-4\delta t^2\alpha_k^2}+1\right)} {}_2F_1\left(\frac{1}{2}\left(\sqrt{1-4\delta t^2\alpha_k^2}+1\right), \frac{1}{2}\left(\sqrt{1-4\delta t^2\alpha_k^2}-2i\delta t\alpha_k^2+1\right); 1-i\delta t\alpha_k^2; -e^{\frac{2t}{\delta t}}\right), \tag{A6}$$

where ${}_2F_1$ denotes the hyper-geometric function. These complex-valued solutions can be rewritten in the form $\epsilon_k^1 = \varepsilon_k + i\zeta_k$, where ε_k and ζ_k can be treated as real and linearly independent equations for each $k = 0, \cdots, N-1$. As evaluated in [57], the solution to Equation (A4) is guaranteed to be of the form:

$$\rho_k(t, \delta t) = \sqrt{A\varepsilon_k^2(t, \delta t)t + 2B\varepsilon(t, \delta t)\zeta_k(t, \delta t) + C\zeta_k^2(t, \delta t)}\,. \tag{A7}$$

In addition, $\Omega_k = \rho_k^2\dot{\gamma_k}$ is an invariant quantity with respect to time. Hence, γ_k can be computed as follows,

$$\gamma_k(t, \delta t) = \int_0^t \frac{\Omega_k}{\rho_i^2(t, \delta t)}dt. \tag{A8}$$

Note that all the quantities are now a function of t and δt; this time dependence is however suppressed in most of this article until necessary. The creation and annihilation operators in Equation (A1) can now be used to construct the invariant operator for each of the N decoupled Hamiltonians of Equation (6):

$$I_k = \Omega_k\left(a_k^\dagger a_k + \frac{1}{2}\right), \tag{A9}$$

where, $k = 0, 1 \cdots, N-1$. Assuming that each invariant operator I_k is one of a complete set of commuting observables for the respective Hamiltonian, H_k, each I_k has its own eigenstates. The ground state for this spectrum of each invariant operator can be computed using the annihilation operator of Equation (A1) by solving $a_k u_{0_k} = 0$. The expression for the ground state for the spectrum of each invariant operator, I_k, of Equation (A9) for each $k = 0, 1 \cdots, N-1$ is given by,

$$u_{0_k} = \left(\frac{\dot{\gamma_k}}{\pi}\right)^{1/4} \exp\left[-\frac{\dot{\gamma_k}}{2}(1 - i\dot{\rho_k}\rho_k\dot{\gamma_k})\tilde{x}_k^2\right]. \tag{A10}$$

The creation operator in Equation (A1) can then be used to evaluate the n^{th} eigenstate of the invariant operator I_k, which is given by,

$$u_{n_k} = \frac{1}{\sqrt{n!}}(a_k^\dagger)^n u_{0_k} = \left(\frac{1}{2^{n_k}n_k!}\right)\left(\frac{\dot{\gamma_k}}{\pi}\right)^{1/4} \exp\left[\dot{\gamma_k}\left(1 - \frac{i\dot{\rho_k}}{\rho_k\dot{\gamma_k}}\right)\tilde{x}k^2\right]\mathbf{H}_{n_k}\left[\sqrt{\dot{\gamma_k}}\tilde{x}_k\right], \tag{A11}$$

where $\mathbf{H}_{n_k}$ denotes the Hermite polynomial of order n_k for each $k = 0, \cdots, N-1$. The eigenstates of the invariant operator shown in Equation (A11) can now be used to compute the wavefunction for each decoupled Hamiltonian of Equation (6), such that $\psi_{n_k} = e^{i\beta_{n_k}} u_{n_k}$, where $\beta_{n_k} = -(1/2 + n_k)$ for $k = 0, \cdots, N-1$.

Appendix B. $\mathcal{C}^{(2)}_{\kappa=1}$ in Terms of Renormalized Parameters

As discussed in [19], one can attempt to find the form of $\mathcal{C}^{(2)}_{\kappa=1}$ by using renormalization. In this subsection, we present an outline of the modified expression for the same in the case of quenched interacting field theory discretized on a d- dimensional lattice containing N oscillators.

The renormalized matrix elements for the A_2 block are given as [19],

$$A_2[m,n] = \frac{a_{mn}\lambda_R \delta^{-d}}{V^{\frac{1}{d-1}} f(\tilde{\omega}_i)}. \tag{A12}$$

Note that all these elements are time-dependent due to the form of frequency $\tilde{\omega}_i$ chosen as a quench profile. The eigenvalues then take the general form [19],

$$\Lambda^{(2)}_i = \frac{b_j \lambda_R \delta^{-d}}{V^{\frac{1}{d-1}} g(\tilde{\omega}_i)}, \tag{A13}$$

where $j \in \{0, 1, \cdots (Dim A_2 - 1\}$ and $i \in \{0, 1, \cdots N-1\}$. As shown in [19], the renormalized penalty factor is,

$$\mathcal{A} = (\lambda_R \delta^{4-d})^{\mu} \delta^{-v} V^{\frac{v}{d-1}}, \tag{A14}$$

where v and μ are arbitrary integers which can be fixed by using physical arguments as discussed in [19]. Using Equation (30), the renormalized complexity contribution for the A_2 block in d- dimensions can then be written as,

$$\mathcal{C}^{(2)}_{\kappa=1} = \frac{(\lambda_R \delta^{4-d})^{\mu} \delta^{-v} V^{\frac{v}{d-1}}}{2} \sum_{k=0}^{d-1} \sum_{i_k=0}^{(\mathrm{Dim}A_2)-1} \left| \log \left(\frac{\Lambda^{(2)}_{i_k} \delta^2}{h_i \tilde{\omega}_{ref} \lambda_0} \right) \right|. \tag{A15}$$

Note that now each $i_k \in \{1, 2, \cdots (\mathrm{Dim}A_2 - 1)\}$ for $k \in \{1, 2, \cdots d-1\}$. Using the renormalized form of eigenvalues from Equation (A13), we finally obtain,

$$\mathcal{C}^{(2)}_{\kappa=1} = \frac{(\lambda_R \delta^{4-d})^{\mu} \delta^{-v} V^{\frac{v}{d-1}}}{2} \sum_{k=0}^{d-1} \sum_{i_k=0}^{(\mathrm{Dim}A_2)-1} \left| \log \left(\frac{b_{i_k} \lambda_R \delta^{2-d}}{V^{\frac{1}{d-1}} g(\tilde{\omega}_i) h_{i_k} \tilde{\omega}_{ref} \lambda_0} \right) \right|. \tag{A16}$$

Note that we have not used this expression to obtain numerically exact results.

Appendix C. Circuit Complexity for Two Oscillators

In Section 4.1, we commented on the ambiguities in fixing the coefficients in the ambiguous A_2 block for an arbitrary number of oscillators, N. Due to these ambiguities, one cannot obtain numerical results for the contribution from the A_2 block in the circuit complexity for N oscillators. However, in this appendix, we choose a minimal basis for the case of two oscillators and hence remove these ambiguities to obtain the total contribution of the A_1 and A_2 blocks in the circuit complexity. We begin by specializing the wavefunction (in normal modes) in Equation (18) to that of two oscillators by inserting $N = 2$, written as:

$$\psi_{0,0}(\bar{x}_0, \bar{x}_1) = \frac{(g_0 g_1)^{1/4}}{\sqrt{\pi}} \exp[-\iota(\gamma_0 + \gamma_1)] \exp[C_0] \exp\Big[-\frac{1}{2}\Big(C_1 \bar{x}_0^2 + C_2 \bar{x}_1^2 + C_3 \bar{x}_0^2 \bar{x}_1^2 + C_4 \bar{x}_0^4 + C_5 \bar{x}_1^4 \Big) \Big]. \tag{A17}$$

The exact form of C_i for $i = 0$ to $i = 5$ can be inferred from the table in Appendix D. Next, we write the above wavefunction in the following form:

$$\psi^s(\bar{x}_0, \bar{x}_1) = \mathcal{N}^s \exp\Big[-\frac{1}{2}\Big(v_a A(s)_{ab}\, v_b\Big)\Big], \tag{A18}$$

where $\mathcal{N}^s$ is the normalization factor. Similar to that of generalized wavefunctions, inserting $s = 1$ into the above equation will correspond to the target state, while inserting $s = 0$ corresponds to the reference state. We choose an unentangled and non-Gaussian reference state given by,

$$\psi^{s=0}(\bar{x}_0, \bar{x}_1) = \mathcal{N}^{s=0} \exp\Big[-\frac{\tilde{\omega}_{ref}}{2}(\bar{x}_0^2 + \bar{x}_1^2 + \frac{\lambda_0}{2}(\bar{x}_0^4 + \bar{x}_1^4 + 6\bar{x}_0^2\bar{x}_1^2))\Big],$$

where λ_0 parameterizes the non-Gaussian nature of the reference state. The exponential in the above equation can be written in form of a matrix $A(s = 0)$ by choosing a basis,

$$\vec{v} = \{\bar{x}_0, \bar{x}_1, \bar{x}_0\bar{x}_1, \bar{x}_0^2, \bar{x}_1^2\}. \tag{A19}$$

The matrix then takes the following form:

$$A(s = 0) = \begin{pmatrix} A_1^0 & 0 \\ 0 & A_2^0 \end{pmatrix}, \tag{A20}$$

where,

$$A_1^0 = \begin{pmatrix} \tilde{\omega}_{ref} & 0 \\ 0 & \tilde{\omega}_{ref} \end{pmatrix} \quad ; \quad A_2^0 = \lambda_0\tilde{\omega}_{ref}\begin{pmatrix} b & 0 & 0 \\ 0 & \frac{1}{2} & \frac{1}{2}(3-b) \\ 0 & \frac{1}{2}(3-b) & \frac{1}{2} \end{pmatrix}.$$

One can choose the values of b such that matrix A_2^0 is non-singular. To diagonalize A_2^0, we set $b = 3$. On the other hand, to choose a non-Guassian reference state, we set $\lambda_0 = 1.5$. Similarly, one can obtain the target state in form of matrix $A(s = 1)$ given by,

$$\psi^s(\bar{x}_0, \bar{x}_1) = \mathcal{N}^{s=1} \exp\Big[-\frac{1}{2}\Big(v_a A(s = 1)_{ab}\, v_b\Big)\Big]. \tag{A21}$$

Choosing the same basis as that in Equation (A19), we can write the matrix for the target state as,

$$A(s = 1) = \begin{pmatrix} A_1^1 & 0 \\ 0 & A_2^1 \end{pmatrix}, \tag{A22}$$

where

$$A_1^1 = \begin{pmatrix} C_1 & 0 \\ 0 & C_2 \end{pmatrix} \quad ; \quad A_2^1 = \begin{pmatrix} \tilde{b}C_5 & 0 & 0 \\ 0 & C_3 & \frac{1}{2}(1-\tilde{b})C_5 \\ 0 & \frac{1}{2}(1-\tilde{b})C_5 & C_4 \end{pmatrix}.$$

The parameter $\tilde{b}$ can be chosen such that A_2^1 is non-singular. Furthermore, to diagonalize A_2^1, we set $\tilde{b} = 1$. It is clear that with a minimal choice of basis given in Equation (A19), one can fix all the elements of both the A_1 and A_2 blocks for the case of two oscillators. Given the expression for circuit complexity for N oscillators given in Equation (30) and setting the penalty factor $\mathcal{A} = \infty$, we have computed the circuit complexity for the two quenched oscillators with quartic coupling by using:

$$\mathcal{C}_{\kappa=1} = \frac{1}{2}\Big(\log\Big|\frac{\det A_1^1}{\det A_1^0}\Big| + \log\Big|\frac{\det A_2^1}{\det A_2^0}\Big|\Big), \tag{A23}$$

where *det* refers to the determinant of the respective block of the matrix. Note that the quench profile chosen as the frequency scale of the system imposes time dependence on each element of the target state matrix block, viz., A_1^1 and A_2^1. The complexity therefore becomes time dependent, this is clearly shown in the numerical results discussed in Section 5.

Appendix D. Tabulated Values of Coefficients

In this appendix, the values of various coefficients we have used in some steps to compute the analytical expression of circuit complexity are tabulated in respective tables.

- We begin by listing the values of B_i for $i = 1, 2...5$ in Equation (19) of Section 3.2 in the Tables A1 and A2.

Table A1. Detailed mathematical structure of the coefficients B_1, B_2, B_3, B_4 and B_5.

B_i	Coefficient of B_i
$B_1(a)$	$-\frac{3x_a^2}{4Ng_aW_a} + \frac{9}{16Ng_a^2W_a} - \frac{x_a^4}{4NW_a}$
$B_2(b,c)$	$-\frac{3x_b^2W_c}{2NW_bg_c(W_b+W_c)} - \frac{3W_bx_c^2}{2Ng_bW_c(W_b+W_c)} + \frac{3}{4Ng_bg_c(W_b+W_c)} + \frac{3W_c}{4Ng_bW_bg_c(W_b+W_c)} + \frac{3W_b}{4Ng_bg_cW_c(W_b+W_c)} - \frac{3x_b^2x_c^2}{N(W_b+W_c)}$
$B_3(d,e)$	$-\frac{12x_dW_ex_e}{Ng_e(W_d+W_e)(W_d+3W_e)} - \frac{4x_dx_e^3}{N(W_d+3W_e)}$
$B_4(f,m,h)$	$-\frac{12x_fx_hW_m}{Ng_m(W_f+W_h)(W_f+W_h+2W_m)} - \frac{12x_fx_hx_m^2}{N(W_f+W_h+2W_m)}$
$B_5(i,j,k,l)$	$-\frac{24x_ix_jx_kx_l}{N(W_i+W_j+W_k+W_l)}$

Note that g_k for $k = 0, \cdots N-1$ is defined in Section 3.1, while W_k is defined in Equation (16). Furthermore, all the indices in the tabulated expressions run from 0 to $N-1$.

- Next, we tabulate the values of coefficients C_i for $i = 1, 2...5$ in Equation (A17) of the Appendix C.

Table A2. Detailed mathematical structure of the coefficients C_1, C_2, C_3, C_4 and C_5.

C_i	Coefficient of C_i
C_0	$\frac{9\lambda}{32g_0^2W_0} + \frac{9\lambda}{32g_1^2W_1} + \frac{3\lambda}{8g_0g_1(W_0+W_1)} + \frac{3\lambda W_1}{8g_0g_1W_0(W_0+W_1)} + \frac{3\lambda W_0}{8g_0g_1W_1(W_0+W_1)}$
C_1	$-\frac{3\lambda}{8g_0W_0} - \frac{3\lambda W_1}{4g_1W_0(W_0+W_1)} - \frac{\nu_0}{2}$
C_2	$-\frac{3\lambda}{8g_1W_1} - \frac{3\lambda W_0}{4g_0W_1(W_0+W_1)} - \frac{\nu_1}{2}$
C_3	$-\frac{\lambda}{8W_0}$
C_4	$-\frac{\lambda}{8W_1}$
C_5	$-\frac{3\lambda}{2(W_0+W_1)}$

Note that $g_k = \gamma_k$, where γ_k for $k = 0, 1$, can be computed by solving the EMP equation as shown in Section 2, while W_k can be computed using Equation (16).

References

1. Calabrese, P.; Cardy, J. Entanglement entropy and quantum field theory. *J. Stat. Mech. Theory Exp.* **2004**, *2004*, 06002. [CrossRef]
2. Witten, E. Notes on Some Entanglement Properties of Quantum Field Theory. *arXiv* **2018**, arXiv:1803.04993.
3. Nishioka, T. Entanglement entropy: Holography and renormalization group. *Rev. Mod. Phys.* **2018**, *90*, 035007. [CrossRef]
4. Blanco, D. Quantum information measures and their applications in quantum field theory. *arXiv* **2017**, arXiv:1702.07384.
5. Headrick, M. Lectures on entanglement entropy in field theory and holography. *arXiv* **2019**, arXiv:1907.08126.
6. Amico, L.; Fazio, R.; Osterloh, A.; Vedral, V. Entanglement in many-body systems. *Rev. Mod. Phys.* **2008**, *80*, 517–576. [CrossRef]
7. Cirac, J.I. Entanglement in many-body quantum systems. *arXiv* **2012**, arXiv:1205.3742.
8. Susskind, L. Three Lectures on Complexity and Black Holes. *arXiv* **2018**, arXiv:1810.11563.
9. Brown, A.R.; Susskind, L.; Zhao, Y.Quantum Complexity and Negative Curvature. *Phys. Rev. D* **2017**, *95*, 045010. [CrossRef]
10. Brown, A.R.; Roberts, D.A.; Susskind, L.; Swingle, B.; Zhao, Y. Holographic Complexity Equals Bulk Action? *Phys. Rev. Lett.* **2016**, *116*, 191301. [CrossRef]
11. Brown, A.R.; Roberts, D.A.; Susskind, L.; Swingle, B.; Zhao, Y. Complexity, action, and black holes. *Phys. Rev. D* **2016**, *93*, 086006. [CrossRef]
12. Susskind, L. Entanglement is not enough. *Fortsch. Phys.* **2016**, *64*, 49–71. [CrossRef]
13. Susskind, L.; Zhao, Y. Switchbacks and the Bridge to Nowhere. *arXiv*, **2014**, arXiv:1408.2823.
14. Stanford, D.; Susskind, L. Complexity and Shock Wave Geometries. *Phys. Rev. D* **2014**, *90*, 126007. [CrossRef]
15. Susskind, L. Computational Complexity and Black Hole Horizons. *Fortsch. Phys.* **2016**, *64*, 24–43. [CrossRef]
16. Jefferson, R.; Myers, R.C. Circuit complexity in quantum field theory. *J. High Energy Phys.* **2017**, *10*, 107. [CrossRef]
17. Hackl, L.; Myers, R.C. Circuit complexity for free fermions. *J. High Energy Phys.* **2018**, *7*, 139. [CrossRef]
18. Chapman, S.; Heller, M.P.; Marrochio, H.; Pastawski, F. Toward a Definition of Complexity for Quantum Field Theory States. *Phys. Rev. Lett.* **2018**, *120*, 121602. [CrossRef]
19. Bhattacharyya, A.; Shekar, A.; Sinha, A. Circuit complexity in interacting QFTs and RG flows. *J. High Energy Phys.* **2018**, *10*, 140. [CrossRef]
20. Polkovnikov, A.; Sengupta, K.; Silva, A.; Vengalattore, M. Colloquium: Nonequilibrium dynamics of closed interacting quantum systems. *Rev. Mod. Phys.* **2011**, *83*, 863–883. [CrossRef]
21. Gogolin, C.; Eisert, J. Equilibration, thermalisation, and the emergence of statistical mechanics in closed quantum systems. *Rep. Prog. Phys.* **2016**, *79*, 056001. [CrossRef] [PubMed]
22. Calabrese, P.; Essler, F.H.L.; Mussardo, G. Introduction to 'quantum integrability in out of equilibrium systems'. *J. Stat. Mech. Theory Exp.* **2016**, *2016*, 064001. [CrossRef]
23. Calabrese, P.; Cardy, J. Quantum Quenches in Extended Systems. *J. Stat. Mech.* **2007**, *706*, P06008. [CrossRef]
24. Basu, P.; Das, S.R. Quantum Quench across a Holographic Critical Point. *J. High Energy Phys.* **2012**, *1*, 103. [CrossRef]
25. Buchel, A.; Lehner, L.; Myers, R.C.; van Niekerk, A. Quantum quenches of holographic plasmas. *J. High Energy Phys.* **2013**, *5*, 067. [CrossRef]
26. Das, S.R.; Galante, D.A.; Myers, R.C. Universal scaling in fast quantum quenches in conformal field theories. *Phys. Rev. Lett.* **2014**, *112*, 171601. [CrossRef] [PubMed]
27. Das, S.R.; Galante, D.A.; Myers, R.C. Universality in fast quantum quenches. *J. High Energy Phys.* **2015**, *2*, 167. [CrossRef]
28. Das, S.R.; Galante, D.A.; Myers, R.C. Smooth and fast versus instantaneous quenches in quantum field theory. *J. High Energy Phys.* **2015**, *8*, 073. [CrossRef]
29. Das, S.R.; Galante, D.A.; Myers, R.C. Quantum Quenches in Free Field Theory: Universal Scaling at Any Rate. *J. High Energy Phys.* **2016**, *5*, 164. [CrossRef]
30. Alba, V.; Calabrese, P. Entanglement dynamics after quantum quenches in generic integrable systems. *SciPost Phys.* **2018**, *4*, 017. [CrossRef]
31. Ghosh, S.; Gupta, K.S.; Srivastava, S.C.L. Entanglement dynamics following a sudden quench: An exact solution. *Europhys. Lett.* **2017**, *120*, 50005. [CrossRef]
32. Ghosh, S.; Gupta, K.S.; Srivastava, S.C.L. Exact relaxation dynamics and quantum information scrambling in multiply quenched harmonic chains. *Phys. Rev. E* **2019**, *100*, 012215. [CrossRef]
33. Camargo, H.A.; Caputa, P.; Das, D.; Heller, M.P.; Jefferson, R. Complexity as a Novel Probe of Quantum Quenches: Universal Scalings and Purifications. *Phys. Rev. Lett.* **2019**, *122*, 081601. [CrossRef] [PubMed]
34. Alves, D.W.F.; Camilo, G. Evolution of complexity following a quantum quench in free field theory. *J. High Energy Phys.* **2018**, *2018*, 29. [CrossRef]
35. Lewis, H.R.; Riesenfeld, W.B. An exact quantum theory of the time-dependent harmonic oscillator and of a charged particle in a time-dependent electromagnetic field. *J. Math. Phys.* **1969**, *10*, 1458–1473. [CrossRef]
36. Adiabatic evolution under quantum control. *Ann. Phys.* **2012**, *327*, 1293–1303. [CrossRef]
37. Ye, M.-Y.; Zhou, X.-F.; Zhang, Y.-S.; Guo, G.-C. Two kinds of quantum adiabatic approximation. *Phys. Lett. A* **2007**, *368*, 18–24. [CrossRef]
38. Choi, J.R. Perturbation theory for time-dependent quantum systems involving complex potentials. *Front. Phys.* **2020**, *8*, 189. [CrossRef]
39. Choudhury, S.; Gharat, R.M.; Mandal, S.; Pandey, N.; Roy, A.; Sarker, P. Entanglement in interacting quenched two-body coupled oscillator system. *Phys. Rev. D* **2022**, *106*, 025002. [CrossRef]

40. Caputa, P.; Das, S.R.; Nozaki, M.; Tomiya, A. Quantum Quench and Scaling of Entanglement Entropy. *Phys. Lett. B* **2017**, *772*, 53–57. [CrossRef]
41. Nielsen, M.A. A geometric approach to quantum circuit lower bounds. *arXiv* **2005**, arXiv:0502070.
42. Nielsen, M.A. Quantum computation as geometry. *Science* **2006**, *311*, 1133–1135. [CrossRef]
43. Dowling, M.R.; Nielsen, M.A. The geometry of quantum computation. *Quantum Info. Comput.* **2008**, *8*, 861–899. [CrossRef]
44. Nielsen, M.A.; Dowling, M.R.; Gu, M.; Doherty, A.C. Optimal control, geometry, and quantum computing. *Phys. Rev. A* **2006**, *73*, 062323. [CrossRef]
45. Yeon, K.H.; Kim, H.J.; Um, C.I.; George, T.F.; Pandey, L.N. Wave function in the invariant representation and squeezed-state function of the time-dependent harmonic oscillator. *Phys. Rev. A* **1994**, *50*, 1035–1039. [CrossRef]
46. Adhikari, K.; Choudhury, S.; Kumar, S.; Mandal, S.; Pandey, N.; Roy, A.; Sarkar, S.; Sarker, P.; Shariff, S.S. Circuit Complexity in $\mathcal{Z}_2$EEFT. *Symmetry* **2023**, *15* , 31. [CrossRef]
47. Parker, D.E.; Cao, X.; Avdoshkin, A.; Scaffidi, T.; Altman, E. A Universal Operator Growth Hypothesis. *Phys. Rev. X* **2019**, *9*, 041017. [CrossRef]
48. Caputa, P.; Liu, S. Quantum complexity and topological phases of matter. *arXiv* **2022**, arXiv:2205.05688.
49. Caputa, P.; Magan, J.M.; Patramanis, D. Geometry of Krylov complexity. *Phys. Rev. Res.* **2022**, *4*, 013041. [CrossRef]
50. Adhikari, K.; Choudhury, S.; Roy, A. $\mathcal{K}$rylov $\mathcal{C}$omplexity in $\mathcal{Q}$uantum $\mathcal{F}$ield $\mathcal{T}$heory. *arXiv* **2022**, arXiv:2204.02250.
51. Adhikari, K.; Choudhury, S. $\mathcal{C}$osmological $\mathcal{K}$rylov $\mathcal{C}$omplexity. *arXiv* **2022**, arXiv:2203.14330.
52. Adhikari, K.; Choudhury, S.; Chowdhury, S.; Shirish, K.; Swain, A. Circuit complexity as a novel probe of quantum entanglement: A study with black hole gas in arbitrary dimensions. *Phys. Rev. D* **2021**, *104*, 065002. [CrossRef]
53. Choudhury, S.; Chowdhury, S.; Gupta, N.; Mishara, A.; Selvam, S.P.; Panda, S.; Pasquino, G.D.; Singha, C.; Swain, A. Circuit Complexity from Cosmological Islands. *Symmetry* **2021**, *13*, 1301. [CrossRef]
54. Eisert, J. Entangling Power and Quantum Circuit Complexity. *Phys. Rev. Lett.* **2021**, *127*, 020501. [CrossRef]
55. Mathur, S.D. Three puzzles in cosmology. *Int. J. Mod. Phys. D* **2020**, *29*, 2030013. [CrossRef]
56. Holzhey, C.; Larsen, F.; Wilczek, F. Geometric and renormalized entropy in conformal field theory. *Nucl. Phys. B* **1994**, *424*, 443–467. [CrossRef]
57. Mukherjee, S.; Choudhury, A.; Guha, P. Generalized damped Milne-Pinney equation and Chiellini method. *arXiv* **2016**, arXiv:1603.08747.